

KINETICS AND MECHANISM OF Ni/ZEOLITE-CATALYZED HYDROCRACKING OF PALM OIL INTO BIO-FUEL

Sri Kadarwati^{1,*}, Fitri Rahmawati², Puji Eka Rahayu¹, Sri Wahyuni¹, and Kasmadi Imam Supardi¹

¹Department of Chemistry, Semarang State University
Bld. D6 level 2, Kampus Sekaran, Gunungpati, Semarang 50229

²PT. Wahana Citra Nabati, Jl. Rawa Sumur I Blok EE/5 Kawasan Industri Pulogadung
Jakarta Timur, 13930

Received January 2, 2013; Accepted March 22, 2013

ABSTRACT

Kinetics and mechanisms of Ni/zeolite-catalyzed cracking reaction of methyl ester palm oil (MEPO) were studied using a continuous flow-fixed bed reactor system at an atmospheric pressure. The catalyst was prepared by wet impregnation method with a solution of nickel nitrate hexahydrate as the precursor and zeolite as carrier. The characteristics of catalyst including active Ni metal content, crystallinity, total acidity, and porosity were evaluated. The reactions were performed with a varied hydrogen flow rate as a carrier gas as well as a reductant and reaction time. Liquid products were analyzed by GC. Analysis by GC-MS was only conducted on a product at hydrogen flow rate with the best conversion. It has been shown that the catalyst has a superior character for hydrocracking reactions of MEPO into green fuel. No considerable effect of hydrogen flow rate on the total conversion was observed. The tests showed that the kinetics of Ni/zeolite-catalyzed cracking reaction followed pseudo-first order kinetics. GC-MS analysis revealed the formation of light hydrocarbon products with C₆-C₈ of aliphatic and cyclic components without oxygenates. Distribution of the product indicated that the cracking reaction as well as the isomerization of the products of hydrocracking occurred. Thus, Ni/zeolite-catalyzed cracking involved cracking/hydrogenation, isomerization, cyclization, and deoxygenation.

Keywords: kinetics; mechanism; palm oil; bio-fuel

ABSTRAK

Kinetika dan mekanisme reaksi perengkahan methyl ester palm oil (MEPO) terkatalisis Ni/zeolite dipelajari dengan reaktor sistem continuous flow-fixed bed pada tekanan atmosfer. Katalis dipreparasi menggunakan metode impregnasi basah dengan larutan nikel nitrat heksahidrat sebagai prekursor dan zeolit sebagai pengemban. Karakteristik katalis yang meliputi kandungan logam aktif Ni, kristalinitas, keasaman total, dan porositas katalis telah dievaluasi. Reaksi dilakukan dengan laju alir hidrogen sebagai gas pembawa sekaligus sebagai reaktan dan waktu reaksi. Produk cair dianalisis dengan GC. Analisis dengan GC-MS hanya dilakukan terhadap product pada laju alir hidrogen dengan konversi terbaik. Telah ditunjukkan bahwa katalis memiliki karakter unggul untuk reaksi hidrorengkah MEPO menjadi bahan bakar nabati. Tidak teramati efek yang signifikan laju alir hidrogen pada konversi total. Hasil uji menunjukkan bahwa kinetika reaksi perengkahan MEPO terkatalisis Ni/zeolite mengikuti kinetika reaksi order satu semu. Analisis GC-MS menunjukkan pembentukan produk hidrokarbon ringan dengan komponen C₆-C₈ alifatik dan siklik tanpa komponen oksigenat. Distribusi produk menunjukkan bahwa reaksi baik perengkahan dan isomerisasi produk hidrorengkah terjadi. Dengan demikian, reaksi perengkahan MEPO terkatalisis Ni/zeolitemelibatkan perengkahan/hidrogenasi, isomerisasi, siklisasi, dan deoksigenasi.

Kata Kunci: kinetika; mekanisme; minyak sawit; bahan bakar nabati

INTRODUCTION

Development of renewable energy is essential along with the depletion of reserves and high oil prices. Catalytic cracking of plant-based oils (vegetable oils) and animal fats as sources of triacylglycerol (TAG) is a natural alternative technique in the production of liquid

fuels based on renewable raw materials. Catalytic cracking of TAG has several advantages that (may) not owned by the esterification-transesterification technique of TAG with methanol a more plural conducted to obtain fatty acid methyl esters as green diesel. These benefits include lower operating costs, compatibility with existing infrastructure, machines and

* Corresponding author. Tel/Fax : +62- 24-8508035
Email address : sri_kadarwati@yahoo.co.id

fuel standards have been developed, and flexibility associated with oil/grease [1].

Indonesia is one of the largest palm oil producers in the world that could potentially be used as a liquid fuel feedstock. By thermal cracking, vegetable oils, animal fat, natural fatty acids and methyl esters of fatty acids such as methyl esters of palm oil at high temperatures produced light hydrocarbon fractions [2]. The fraction of these light hydrocarbons is bio-gasoline in a greater percentage than the percentage of biodiesel. Because palm oil mainly contains palmitic acid (16:0) and oleic acid (18:1), the methyl ester of palm oil can be used as an alternative clean fuel engine [3].

The catalyst with mesoporous pores, high ratio of Si/Al, and high surface area is very effective in the termination reaction of long chain carbon in palm oil to produce compounds of diesel fuel fractions, and even to the gasoline fraction [4]. Catalytic conversion of palm oil using a composite micro-mesoporous zeolite catalyst in fixed bed reactor system operated at a temperature of 450 °C produced gasoline product of 48 w.t.% and of 99 w.t.% of palm oil was converted [5]. Catalytic cracking of palm oil using a fixed bed reactor and catalyst HZSM-5 at a temperature of 400 °C produced hydrocarbons in the gasoline fraction up to 40–70% with the two main reactions involving namely cracking and deoxygenation [6] with high selectivity towards aromatic compounds and a little coke deposition [7].

Catalytic cracking using Ni/zeolite catalysts with nitrogen as a carrier gas only yielded 27.5% of gasoline and 36.08% of diesel fractions [8]. Thus, the use of hydrogen as a carrier gas as well as a reactant in this study was a good effort.

Catalytic conversion of palm oil into bio-gasoline catalyzed by Ni/zeolite [9] reached an optimum condition at temperature of 450 °C with Ni/zeolite (2% of Ni content) catalyst with a conversion of 100% and a yield of 18% bio-gasoline. Several factors affecting the catalytic cracking reaction are important to be investigated. To achieve the goal, a study about the reaction kinetics and mechanism of the catalytic cracking of palm oil into bio-gasoline is presented in this paper.

EXPERIMENTAL SECTION

Materials

Indonesian natural zeolite was provided by PT. Zeolita Prima (Yogyakarta, Indonesia). The zeolite was prepared by washing using distilled water (Chemistry Lab., Semarang State University) and filtering them using a particulate filter (anonymous). To activate the zeolite 1% of HF (85%, E. Merck) solution, 6 N of HCl (37%, E Merck) solution, and 1.0 M NH₄Cl (99.8%, E. Merck) solution, respectively, were used. Palm oil was

purchased from a traditional market in Semarang, Central Java as a crude frying oil. Methyl ester palm oil (MEPO) was prepared by reacting the oil with potassium methoxide produced from the reaction between KOH (99.5%, E. Merck) and methanol (99.8%, E. Merck). Ni/zeolite catalyst was prepared by impregnation method using nickel nitrate hexahydrate Ni(NO₃)₂·6H₂O (E. Merck) as the metal precursor. Hydrogen, nitrogen, and oxygen of 99.9% purity were provided by PT. Samator Gas (Semarang, Central Java). The total acidity of Ni/zeolite catalyst was determined by adsorption method using NH₃ (25%, E. Merck).

Instrumentation

Ni/zeolite catalyst prepared was analyzed for the Ni content using Atomic Absorption Spectrophotometer Perkin Elmer Analyst-100, the crystallinity using XRD PW3373 PANAnalytical, and the porosity properties using a Surface area analyzer NOVA 1200e. All of the reaction performed in this research used a continuous-flow fixed bed reactor. Products obtained at the end of reactions were analyzed by using Gas Chromatograph GC Agilent Technologies 6820 equipped with an HP5 semipolar column (30 m length, 0.32 mm diameter), and FID detector. The product which had the highest fraction of bio-gasoline was analyzed using Gas Chromatograph QP2010S SHIMADZU equipped with MS detector, a Rastek RXi-5MS column (30 m length, 0.25 mm internal diameter), and He as the carrier gas.

Procedure

Preparation of catalysts

Zeolite support (100 mesh) was prepared by grinding, washing, and filtering. Activation of zeolite was performed by using a method reported elsewhere [20]. A 1% HF solution, a 6 N HCl solution, and a 1 M NH₄Cl solution were used. Zeolite was soaked in a 1% HF solution with a ratio of 1:2 by mass in a plastic container for 10 min at room temperature. Subsequently, the zeolite was filtered and washed until reached pH of 6. After dried, the zeolite was refluxed and stirred in a 6 M HCl solution for 30 min at 90 °C. Subsequently, it was filtered and washed using aquadest until reached pH of 6. A treatment with a 1 M NH₄Cl solution was conducted within seven days at 90 °C with a 3 h thermal treatment and an every-hour shake each day. Finally, it was filtered and washed with aquadest until reached pH of 6, and dried in an oven at 120 °C for 12 h.

Ni zeolite catalysts were prepared by a wetness impregnation with aqueous solution of Ni(NO₃)₂·6H₂O. The metal loading was 2% of the weight of zeolite. The

zeolite support was soaked in the metal precursor solution at 90 °C for 3 h. The obtained catalyst was then dried in an oven at 120 °C for 24 h, and ground to 100 mesh in particle size. Finally, the catalyst sample was calcined using nitrogen at 500 °C for 3 h, oxidized at 500 °C for 2 h, and reduced at 500 °C for 2 h.

Characterization of catalysts

Ni/zeolite catalyst was characterized by using atomic absorption spectrophotometer Perkin Elmer Analyst-100 for determining Ni content. The analysis on a PW3373 PANAnalytical X-ray diffractometer using Cu K α ($\lambda = 0.154$ nm) radiation was performed to observe the catalyst crystallinity. The diffraction patterns were recorded by scanning 2θ angles from 3° to 80° at 300 °C until the sample achieved quasi equilibrium state as evidenced from the absence of noticeable changes in the diffraction patterns. The average particle size of the catalysts was determined using Scherrer equation [10]. Total acidity of catalyst was determined using gravimetric method using ammonia as an adsorbate. Catalyst porosity was determined using a NOVA 1200e Gas Sorption Analyzer. Specific surface area of catalyst was calculated using Brunauer, Emmet, and Teller (BET) method, whereas total pore volume and average pore radius were calculated using Barrett, Joyner, Halenda (BJH) method.

Catalytic cracking of MEPO with Ni/zeolite catalyst

A one gram of Ni/zeolite catalyst was packed in a fixed bed reactor column and heated up to 450 °C. Hydrogen was flowed (10 mL/min to 50 mL/min) through the evaporator contained MEPO. The evaporator was then heated up so that the MEPO vaporized and flowed together with hydrogen into the reactor. The reactions were conducted for 30 to 90 min. The products were collected and analyzed by using Gas chromatograph. The product with the highest conversion was analyzed using GC-MS.

Kinetics of Ni/zeolite-catalyzed cracking of MEPO is based on Langmuir-Hinshelwood reaction mechanism assuming that the reaction follows the pseudo-first order reaction kinetics. The measurement of rate of reaction in a flow-fixed bed reactor was performed at a constant intersection area, a certain reactant flow rate passing through a constant bulk volume of catalyst dV with the concentration of i element introducing an unit is C_i , and the concentration leaving an unit is $C_i + dC_i$, then the kinetics approach for the rate of reaction r_i can be expressed as

$$\frac{dn_i}{dt} = r_i dV - u dC_i \quad (1)$$

Assuming that the reaction undergoes in steady-state condition and enclosed system, the rate constant at t can be determined using the equation

$$k = \frac{u}{V} \ln \frac{C_0}{C} \quad (2)$$

k is the rate constant of the formation of C₅-C₁₁ fraction, u is the reactant flow rate (mL/min), V is the bulk volume of catalyst (mL), C and C_0 are the concentration of products leaving the reactor and the concentration of MEPO entering the reactor, respectively. Briefly, V/u can replace t variable [11].

RESULT AND DISCUSSION

Characteristics of Ni/Zeolite Catalyst

Porosity of Ni/zeolite catalyst

In a catalytic reaction, the contact between the larger methyl ester of palm oil and the active site of the catalyst must occur. The higher the surface area of the catalyst, the greater the chance of cracking reaction. In addition, the large size of the pore radius will give a better chance for molecules to pass through in order to reach the active sites.

Table 1 shows that the surface area and pore volume of Ni/zeolite catalyst was greater than that of the natural zeolite and activated natural zeolite (H-zeolite), while its average pore radius was the smallest compared to other catalysts that have been prepared. This suggests that physically Ni/zeolite catalyst was superior in terms of its porosity characteristics. The expected physical characteristic is high surface area and large pore volume, but with small average pore radius. That is because the presence of a high surface area and large pore volume allows for more active sites which promote more interactions between the feed and the catalyst. For the similar reason, the smaller average pore radius gives the shorter distance between Ni metals, increasing the number of the active sites of the catalyst due to the new pore formation.

Number of acid sites of Ni/zeolite catalyst

Catalyst performance is strongly influenced by the acidity of the catalyst. A large number of active sites results in the higher adsorption energy towards the reactants that means the more cracked feed into biogasoline. To determine the number of acid sites at the catalyst surface, the adsorption of basic adsorbate was carried out. The number of acid sites with ammonia as the basic adsorbate is the total number of acid sites on the assumption that the small NH₃ molecules can go up into the pores of the catalyst.

The acidity is critical in determining the number of active sites; the greater the acidity, the more the active sites. An increase in the number of acid sites of Ni/zeolite catalyst (11.09×10^{-4} mmol NH₃/g) compared to the original zeolite (9.42×10^{-4} mmol NH₃/g) and H-zeolite (1.27×10^{-4} mmol NH₃/g) is shown in Table 2.

Table 1. Porosity of catalysts

Catalyst	Specific surface area (m ² /g)	Average pore radius (Å)	Total pore volume (cc/g)
Zeolite	35.08	40.09	70.33 x 10 ⁻³
H-Zeolite	44.55	52.11	116.1 x 10 ⁻³
Ni/Zeolite	90.5611	31.11	141.0 x 10 ⁻³

Table 2. Number of acid sites of catalysts

Catalyst	Total number of acid sites (moles/g)
zeolite	9.42 x 10 ⁻⁴
H- zeolite	1.27 x 10 ⁻⁴
Ni/zeolite	11.09 x 10 ⁻⁴

Table 3. Ni content in Ni/zeolite catalyst

Measured result with AAS (ppm)	Loaded Ni (g)	Impregnated Ni (g)	Efficiency (%)
397.6	0.8	0.7952	99.4

Table 4. Data of Theta and first-three highest peaks of zeolite, H-zeolite, and Ni/zeolite

Catalyst	Theta	FWHM (deg)	Particle size (nm)	Average particle size (nm)
Zeolite	12.9699	0.257	29.77	13.23
	11.2908	0.3405	7.11	
	14	0.4044	2.81	
H-Zeolite	1302095	0.2602	28.73	16.51
	1411	0.417	0.54	
	13.46	0.2572	20.27	
Ni/Zeolite	12.94645	0.2608	29.62	19.29
	13.38	0.2538	22.52	
	4.9422	0.33133	5.72	

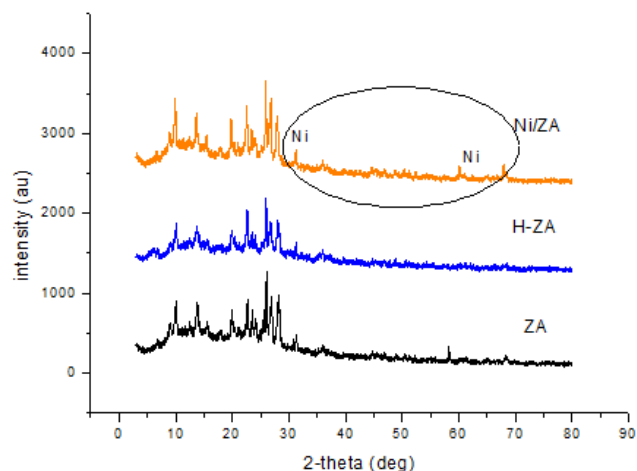
This might be because of the loaded Ni metals at the catalyst surface which resulted in an increase in the partially-charged orbitals of Ni metals which is effective to accept an electron pair from a basic adsorbate. Thus, Ni/Zeolite catalyst also provided a superior characteristic based on the number of acid sites.

Ni content in Ni/zeolite catalyst

It has been argued that the quality of a catalyst is determined by the quality of metal dispersion on the support, while the dispersion quality is influenced by the metal content [12]. Therefore, the test to determine the amount of Ni content in the catalyst is of importance. The distributions of Ni metal in the catalyst are presented in Table 3, showing that the efficiency of Ni loading on Ni/zeolite was 99.4%.

Crystallinity and particle size of Ni/zeolite catalyst

Crystallinity and particle size of Ni/zeolite catalysts can be justified from the results of XRD analysis. These analyses were performed on Ni/zeolite catalyst, acid treated zeolite (H-zeolite), and zeolite. Based on Fig. 1 it can be seen that the crystallinity of zeolite after entrusting of Ni metal was still as high as before. This was shown by the data of 2-theta of catalyst diffraction

**Fig 1.** Diffraction patterns of zeolite, H-zeolite, and Ni/zeolite

patterns. However, a decrease and increase in 2-theta peaks indicating the presence of Ni metal impregnated on Ni/zeolite were observed. Thus one can say that the impregnation of Ni metal did not lower the crystallinity of zeolite. Ni metal is located at 2 theta of 32.36° and 65.96°.

In addition, the crystallinity of catalyst can also be observed through the three highest peaks of each of the solids of diffraction patterns. Table 4 also presents the average particle size of each sample catalyst which has been determined using Scherrer equation [10].

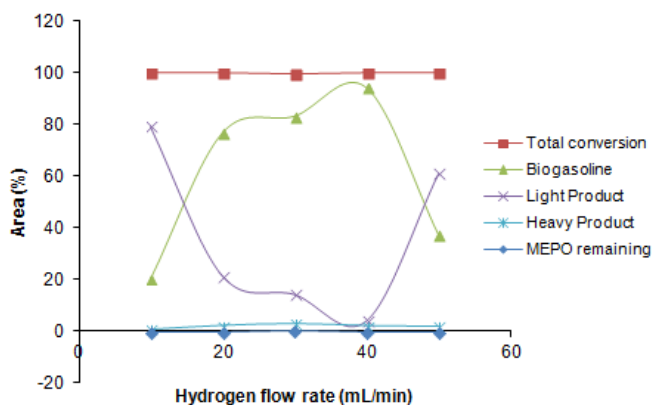
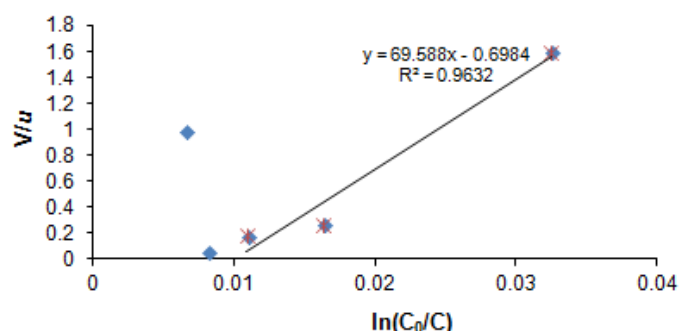
Catalytic Cracking of MEPO Catalyzed by Ni/Zeolite

Activity of Ni/zeolite catalyst: effect of hydrogen flow rate

Total conversions (Table 5 and Fig. 2) of products of the cracking were determined from the amount of product that converted from methyl ester palm oil. Determination of total conversions was based on the percentage of peak area on chromatograms of cracking products. The products of catalytic cracking of palm oil in this study were restricted on biogasoline hydrocarbon fraction with a number of carbon atoms of C₅-C₁₁. In this study, the gas product and coke yield

Table 5. Bio-gasoline fraction at various hydrogen flow rate

H ₂ flow rate (mL/min)	Total conversion (%)	C ₅ -C ₁₁ Bio-gasoline fraction (%)	Light gas fraction (%)	Heavyoil fraction (%)	MEPO remaining (%)
10	100.00	20.11	79.18	0.69	0
20	100.00	76.60	21.27	2.13	0
30	99.61	83.02	14.15	2.82	0.39
40	100.00	94.03	3.88	2.09	0
50	100.00	37.30	60.94	1.76	0

**Fig 2.** Product distribution of Ni/zeolite-catalyzed hydrocracking of MEPO at various hydrogen flow rates**Fig 3.** Plot of V/u versus $\ln(C_0/C)$ for pseudo-first order kinetics

were undetermined.

Hydrogen flow rate had no significant effect on the total conversion of Ni/zeolite-catalyzed cracking reaction of MEPO zeolite at a temperature of 450 °C, as well as on the heavy fractions and uncracked MEPO. However, the hydrogen flow rate significantly affected the yield of C₅-C₁₁ fraction and light fractions. The produced C₅-C₁₁ fraction increased with increasing flow rate up to 30 mL/min. The higher flow rate the higher amount of hydrogen as a carrier gas as well as the reactants. Thus, the amount of MEPO steam and hydrogen entering the reactor and react on the catalyst surface also increased.

Hydrogen flow rate is inversely proportional to the residence time of reactant molecules on the surface of the catalyst. The higher the flow rate, the smaller the residence time of reactant molecules on the surface of the catalyst. This strongly affects the probability of a

reaction; the smaller residence time, the smaller the opportunity of reactant molecules to interact and produce the products. It was observed at a flow rate of 50 mL/min which had lower C₅-C₁₁ fraction compared to lower hydrogen flow rates. Furthermore, it seems that extreme residence time, either very high at hydrogen flow rate of 10 mL/min or very low at that of 50 mL/min, would show a similar trend for product distribution (less gasoline and heavy fraction, more light fraction). It might have different reasons; lower hydrogen flow rate (10 mL/min) provided more interactions and suitable length of time for the reactants to be converted to products, whereas higher one gave more hydrogen as the reductant to hydrogenate the MEPO during the reaction.

The fraction of light oil produced from the Ni/zeolite-catalyzed cracking reaction of MEPO has the opposite trend to the formation of the C₅-C₁₁ fraction. The increase in hydrogen gas flow rate up to 30 mL/min, the amount of light oil fraction decreased due to the limited amount of hydrogen supplied to the reaction system. Hydrogen is only sufficient to saturate the double bond and crack the MEPO molecules to a smaller fraction but not too light. The supply of hydrogen which was more than 30 mL/min enabled the hydrogenation of double bonds and the hydrocracking of MEPO molecules to much lighter fractions.

As the flow rate of hydrogen only affected significantly to the C₅-C₁₁ and the light oil fractions, the kinetic approach used i.e. the pseudo-first order reaction kinetics only considered the rate of formation of the C₅-C₁₁ fraction (Fig. 3). In addition, the kinetics model was only valid for low hydrogen flow rate (≤ 30 mL/min). For the range of hydrogen flow rate, the Ni/zeolite-catalyzed cracking reaction of MEPO at a temperature of 450 °C followed pseudo-first order reaction kinetics with the rate constant (k) of 69.58 min⁻¹. The reaction rate constant was the constant rate for formation of C₅-C₁₁ fraction.

Effect of reaction time to catalyst activity

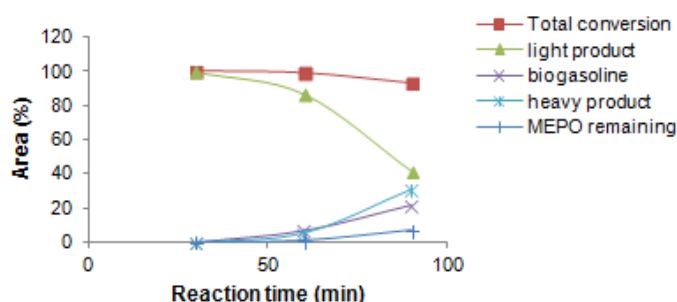
Reaction time significantly affected to all fractions produced in the catalyzed cracking reaction of MEPO, as well as to MEPO molecules which have not been cracked (Table 6 and Fig. 4). Cracking reactions with variation of reaction time were performed at a flow rate

Table 6. Bio-gasoline fraction at various reaction times

Reaction time(min)	Total conversion (%)	C ₅ -C ₁₁ Bio-gasoline fraction (%)	Light gas fraction (%)	Heavyoil fraction (%)	MEPO remaining (%)
30	99.94	0.27	99.50	0.11	0.06
60	98.92	6.83	86.56	5.53	1.08
90	93.22	21.34	41.07	30.80	6.78

Table 7. Composition of organic liquid product at 500°C and 40 mL/min of H₂ flow rate

Retention time (min)	Area (%)	Mr (g/mol)	Compound suspected
2.583	15.310	86.0	2-methyl pentane
2.645	14.810	86.0	3-methyl pentane
2.718	18.910	86.0	n-hexane
2.912	16.360	84.0	Methyl cyclopentane
3.192	0.850	84.0	cyclohexane
3.267	0.020	100.0	2,3-dimethyl pentane
3.482	23.820	114.0	Iso-octane
3.531	9.760	98.0	4-methyl-1-hexene
3.881	0.170	114.0	2,2-dimethyl hexane

**Fig 4.** Product distribution of Ni/zeolite-catalyzed hydrocracking of MEPO at various reaction times

of 40 mL/min as this flow rate was capable of producing the highest fraction of C₅-C₁₁ at the range of hydrogen flow rate which has been studied. The increase in reaction time, total conversion and light fraction decreased significantly while the C₅-C₁₁ fraction, heavy fraction, and the MEPO fractions which have not been cracked increased considerably. This is probably caused by a decrease in catalytic activity due to the prolonged reaction time. The decrease in catalytic activity may be caused by coke deposition that covers the active site of the catalyst. This resulted in a decrease in total conversion because not all of MEPO molecules at fluid phase can be adsorbed on the catalyst active sites for further reaction with hydrogen.

The prolonged reaction time can also cause polymerization reaction of cracking products generated to a heavy fraction despite increased reaction time will also provide greater opportunities for the cracking products to perform isomerization reaction to more stable products and give more opportunities to the partially-cracked products to be completely cracked. However, cracking in the prolonged reaction time will

also trigger the formation of more light products which is not desired.

GC-MS Analysis and Hypothetical Mechanism

The mechanism of Ni/zeolite-catalyzed cracking was planned to be studied by changing intensity and position of absorption in FT-IR spectra. However, due to the catalyzed cracking reactions often involve deoxygenation by releasing water as a byproduct [13] as a result of simultaneous dehydration and decarboxylation reactions on zeolite-based catalyst [14], the hypothetical mechanism of Ni/zeolite-catalyzed cracking was studied based on compounds detected by GC-MS. The presence of water can damage the NaCl window plate which was used in FT-IR analysis.

To find out what compounds contained in the reaction product of Ni/zeolite-catalyzed hydrocracking, an analysis of the product in the best condition (temperature of 450 °C and hydrogen flow rate of 40 mL/min) using GC-MS (Shimadzu QP2010S, with Rxi Rastek-5MS column, 30 m long, 0.25 m ID) was performed. The results are presented in Table 7.

Brønsted and Lewis acid sites at Ni/zeolite catalyst surface allow the hydrogenation process that result directly in the cracking process. The high content of acid sites at the catalyst surface causes continuous hydrocracking so that the products detected by GC-MS were mostly light hydrocarbon products of C₆-C₈ without any oxygenated product. This was supported by the appearance of a sample containing water as a byproduct of the deoxygenation reaction. Product distribution in Table 7 indicates that the cracking reaction as well as the isomerization of the products of hydrocracking occurred. This is also shown by the

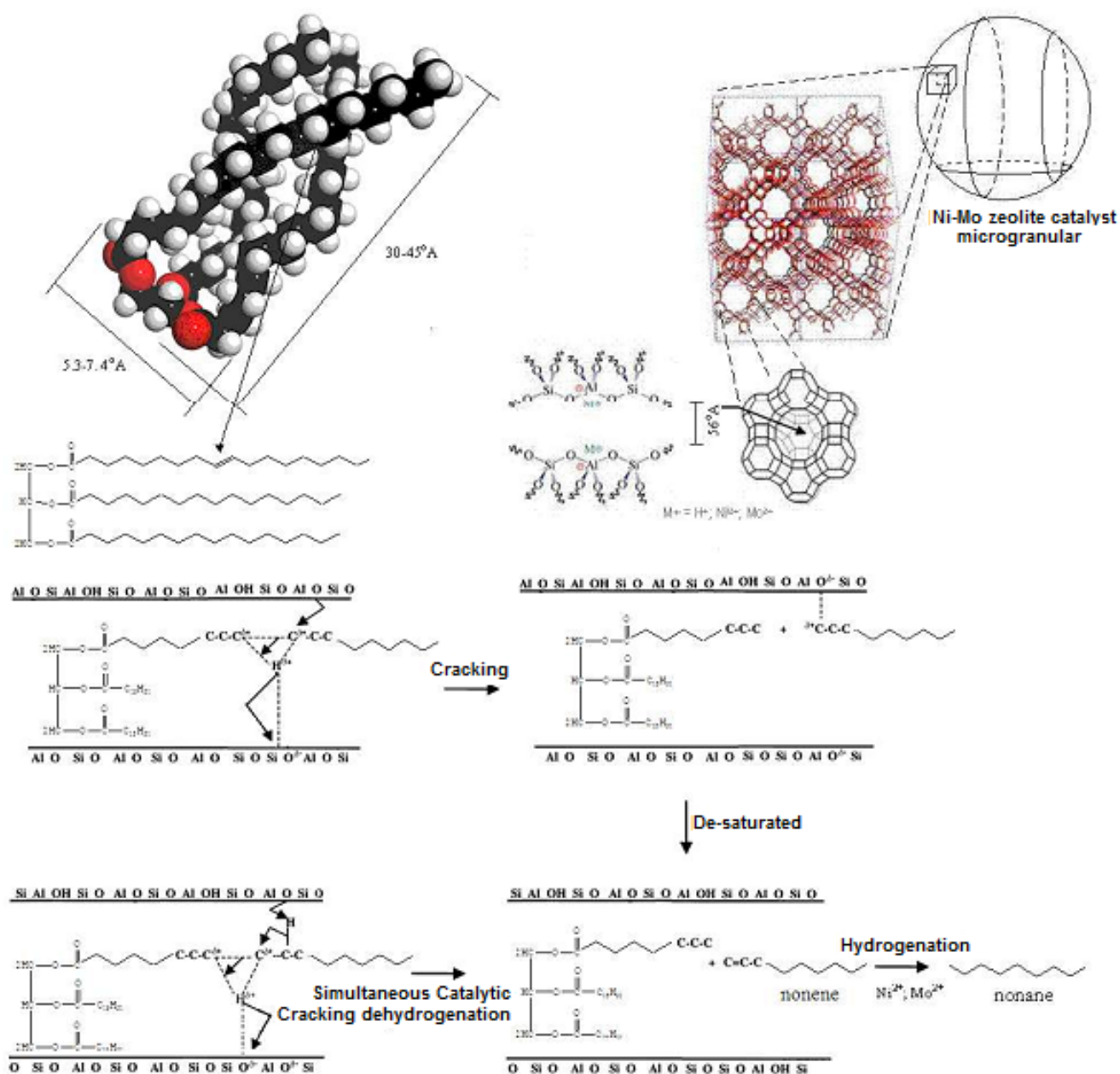


Fig 5. Reaction mechanisms of Ni/zeolite-catalyzed hydrocracking of MEPO into bio-fuel adopted from Nasikin et al. [18]

dominance of isoparaffinic compounds than n-paraffinic compounds in biogasoline fraction. This is made possible by the ability of zeolites to catalyze the isomerization reaction compared to another carrier such as alumina [15]. Aromatics products which usually dominate the catalyzed hydrocracking of palm oil as reported Siregar and Amin [16] did not happen. In this study only saturated cyclic products were found. This is because the cracking reaction with zeolite-based catalyst can accommodate isomerization reactions, cracking and cyclization simultaneously [15].

Table 7 also shows that all the products detected by GC-MS were a product of the number of carbon atoms in the range of biogasoline. Thus it can be said that 100% of the products produced at a temperature of 450 °C and hydrogen flow rate of 40 mL was a biogasoline fraction. Thus the biogasoline yield in this study was 100%. This is a bit contrary to the results of measurements with the GC in Table 5 and Fig. 2. Table 5 states that only 94.03% of the total conversion of 100% of Ni/zeolite-catalyzed cracking of MEPO was a biogasoline fraction. A 3.88% of them were very light

fraction ($C < 5$) whereas a 2.09% was the heavy fraction ($C > 11$). It seems that the storage factor affects the existence of very light fraction with a very low boiling point as it can easily evaporate from the sample. However, the explanation of undetectable heavy fraction by GC-MS is still not clear even though the heavier MEPO fraction than heavy oil products can still be detected by GC-MS.

The high yield biogasoline fractions generated in this study could be very promising for the exploration of green gasoline as a renewable energy resource. Wijanarko et al. [17] reported that the yield of gasoline fraction obtained from catalyzed cracking of palm oil by γ -alumina was 45.4% with the remains were heavy residue fraction. This suggests that Ni/zeolite-catalyzed cracking of MEPO was at very high selectivity towards gasoline fraction due to the bifunctional properties of Ni/zeolite catalyst. It has been well-known that Ni metals are able to catalyze hydrogenation and oxygenation reaction, while zeolite is a hydrocracking catalyst that has been used extensively in the petroleum industry.

Methyl ester of palm oil contains fatty acids in major including myristic acid, palmitic acid, and oleic acid. The proposed reaction mechanism refers to the cracking mechanism of palm oil into gasoline fractions that have been proposed by Nasikin et al. [18]. The catalyst is expected to break the double bond in oleic acid because such bonds are more easily broken than a single bond. In this case, the methyl ester molecules can enter the pores of the catalyst with a diameter of $\pm 0.56^\circ\text{A}$ due to the longitudinal diameter (approximately 5.3 to 7.4°A) and the length of MEPO chain (about 30 – 45°A) are smaller than the pore of the catalyst. Unsaturated molecules such as methyl ester of oleic acid are undesirable in fuels because it is prone to react with the impurities present in the fuel or even with the methyl ester of oleic acid molecules to form other unintended polymers [19].

The expected reaction mechanism is presented in Fig. 5. Idem et al. [19] proposed that before the fraction of light hydrocarbons (C_2 – C_{10}) were formed, methyl esters or triglycerides of palm oil will be going through the process of cracking due to thermal effects first to form heavier fractions of hydrocarbons (C_{12} – C_{20}). After thermally cracking occurs, then catalyzed cracking occurs by changing the heavier fraction to lighter fractions.

CONCLUSION

Active metal impregnation of nickel on the surface of zeolite gave rise to the surface area and total pore volume respectively 2.5 times and 2 times greater than the acid-treated zeolite with the average pore radius decreased by 22.5%. The high Ni metal impregnation

efficiency on the surface of zeolite increased total zeolite acidity by 22%. Impregnating active metal Ni did not affect the crystallinity of the support, but lowers the average size of catalyst particles by 13% of the average particle size of the support.

Hydrogen flow rate had no significant effect on the total conversion of Ni/zeolite-catalyzed cracking reaction of MEPO at a temperature of 450°C but significantly affected on the C_5 – C_{11} and light oil fractions. The rate of formation of C_5 – C_{11} fraction followed pseudo-first order kinetics with a rate constant of formation of C_5 – C_{11} fraction (k) of 69.58 min^{-1} .

Dominant products detected by GC-MS were light hydrocarbon products of C_6 – C_8 aliphatic and cyclic components without oxygenates. Distribution of the product indicated the cracking reaction as well as the isomerization of the products of hydrocracking. Thus, the cracking reaction of MEPO catalyzed by Ni/zeolite involved cracking reaction/hydrogenation, isomerization, cyclization, and de-oxygenation.

ACKNOWLEDGEMENT

The authors would like to thank to Faculty of Mathematics and Natural Sciences Semarang State University for funding this research through Research/Study Group-Based Research Grant 2012.

REFERENCES

1. Stumborg, M., Wong, A., and Hogan, E., 1996, *Bioresour. Technol.*, 56, 1, 13–18.
2. Gaya, J.C.A. 2003, *Biodiesel from Rape Seed Oil and Used Frying Oil in European Union*, Copernicus Institute, Universiteit Utrecht.
3. Demirbas, A., 2003, *Energy Sources*, 25, 457–466.
4. Twaiq, F.A., Zabidi, N.A.M. and Bhatia, S., 2003, *Microporous Mesoporous Mater.*, 64, 1-3, 95–108.
5. Sang, O.Y., 2003, *Energy Sources*, 25, 9, 859–869.
6. Leng, T.Y., Mohamed, A.R., and Bhatia, S., 1999, *Can. J. Chem. Eng.*, 77, 1, 156–162.
7. Twaiq, F.A., Zabidi, N.A.M. and Bhatia, S., 1999, *Ind. Eng. Chem. Res.*, 38, 9, 3230–3237.
8. Handoko, D.S.P., 2006, *Jurnal Ilmu Dasar*, 7, 1, 42–51.
9. Kadarwati, S., and Wahyuni, S., 2011, *Proceeding Seminar Nasional Kimia dan Pendidikan Kimia III*, ISBN 978-979-1533-85-0, 297–308.
10. Scherrer, P., 1918, *Mathematisch-Physikalische Klasse*, 2, 98–100.
11. Moore, J.W., and Pearson, R.G., 1981, *Kinetics and Mechanisms*, 3rd Ed., John Wiley and Sons, Inc., Canada.

12. Trisunaryanti, W., Triwahyuni, E., and Sudiono, S., 2005, *Teknoin.*, 10, 4, 269–282.
13. Zabeti, M., Nguyen, T.S., Lefferts, L., Heeres, H.J., and Seshan, K., 2012, *Bioresour. Technol.*, 118, 374–381.
14. Moens, L., Black, S.K., Myers, M.D., and Czernik, S., 2009, *Energy Fuels*, 23, 5, 2695–2699.
15. Sotelo-Boyás, R., Liu, Y., and Minowa, T., 2011, *Ind. Eng. Chem. Res.*, 50, 5, 2791–2799.
16. Siregar, T.B., and Amin, N.A.S., 2006, *Jurnal Teknologi*, 44, F, 69–82.
17. Wijanarko, A., Mawardi, D.A., and Nasikin, M., 2006, *Makara J. Technol. Ser.*, 10, 2, 51–60
18. Nasikin, M., Susanto, B.H., Hirsaman, M.A., and Wijanarko, A., 2009, *World Appl. Sci. J.*, 5, 74–79.
19. Idem, R.O., Katikaneni, S.P.R., and Bakhsi, N.N., 1997, *Fuel Process. Technol.*, 51, 101–125.
20. Trisunaryanti, W., Triyono, and Fibirna, D.A., 2003, *Indo. J. Chem.*, 3, 2, 80–90.